View metadata, citation and similar papers at core.ac.uk
brought to you by CORE
provided by PUblication MAnagement

Computer Methods in Biomechanics and Biomedical Engineering
Vol. 00, No. 0, 2011, 1–10

Taylor & Francis
Taylor & Francis Group

Q4 Interaction between the septum and the left (right) ventricular free wall in order to evaluate the effects on coronary blood flow: numerical simulation

Claudio De Lazzari[a,b]*

[a]*C.N.R., Institute of Clinical Physiology, U.O.S. of Rome, Italy;* [b]*National Institute of Cardiovascular Research, Bologna, Italy*

(*Received 28 January 2011; final version received 13 June 2011*)

Mathematical modelling of the cardiovascular system (CVS) can help in understanding the complex interactions between both the ventricles and the septum. By describing the behaviour of the left (right) ventricular free wall, atria and septum using the variable elastance models, it is possible to reproduce their interactions. By relating the mechanical properties of both atria and both ventricles to the electrocardiogram (ECG) signal, it is possible to analyse the effects produced by Q1 different ECG delay on haemodynamic parameters. In the cardiovascular field, the incorrect interactions between septum and both ventricular free walls are based on many pathological conditions, i.e. symptomatic heart failure resulting from systolic dysfunction, ischemic dilated cardiomyopathy, and so on. The possible corrections that can be induced on the QRS complex duration in the ECG signal (i.e. cardiac resynchronisation therapy, CRT) can produce benefits improving the clinical status of the patient. The aim of this work was to evaluate, using our numerical simulator of the CVS, the effects induced on coronary blood flow (CBF) and aortic pressure using different ECG times, intra-ventricular and inter-ventricular delays. The results were obtained by reproducing the circulatory baseline and CRT conditions of seven patients described in literature. Haemodynamic simulated results are in accordance with literature data. Also the controversial results on CBF, in presence of CRT, are consistent with those described in the literature.

Keywords: circulatory system; haemodynamics; coronary circulation; left ventricle; computer simulation; cardiac resynchronisation therapy

Introduction

In the heart dysfunction study, many pathological conditions are due to inter-ventricular and/or intra-ventricular dyssynchrony. Many patients with advanced heart failure (HF) exhibit significant intra-ventricular or inter-ventricular conduction delays (IVCD) that disturb the synchronous beating of the ventricles so that they pump less efficiently (Edvardsen et al. 2005; Kalogeropoulos et al. 2008). Ventricular dyssynchrony can produce a number of deleterious effects on cardiac function such as reduced diastolic filling time, weakened contractility, protracted mitral regurgitation and post-systolic regional contraction.

The possible corrections that can be induced to solve the ventricular dyssynchrony – i.e. the reduction in the QRS complex duration in electrocardiogram (ECG) signal (i.e. cardiac resynchronisation therapy, CRT) – can produce benefits improving the clinical status of the patient (Rinaldi et al. 2002; Ghio et al. 2004; Kamdar et al. 2010).

In the literature, it has been reported that the mechanisms of ventricular interaction can be divided into two types of interactions. The first one (called 'in series' interaction) is caused by the outlet of each ventricle that is connected to the inlet of the other ventricle through the systemic/pulmonary circulation. The second one (called 'direct' interaction) is connected to the septum wall, shared by left and right ventricles and the pericardium that contains the heart. The relative contributions of these types of interaction are difficult to measure (Slinker and Glantz 1986).

A numerical model of the cardiovascular system (CVS) can be a useful tool to help understand the complex interactions between the left (right) ventricular free walls, Q1 atria and septum. This paper describes the updating of the numerical simulator of the CVS, CARDIOSIM© (Ferrari et al. 1992; De Lazzari et al. 1994), implementing the behaviour of the septum that permits to simulate all interactions between the two ventricular chambers. In the simulator, the different circulatory districts were represented by a lumped parameter model; both ventricular and atrial functions were implemented using a variable elastance model (Maughan et al. 1987; Sagawa et al. 1988; De Lazzari et al. 2009). The behaviour of the septum was simulated using a variable elastance model (Maughan et al. 1987). An updated software was used to study, on the coronary blood flow (CBF)-systemic aortic pressure (AoP) plain, the CBF–AoP loops (De Lazzari et al. 2009) in correspondence to different ECG times, intra-ventricular and inter-ventricular delays.

The results obtained showed that the software simulator CARDIOSIM© can reproduce the pathological conditions of patients with idiopathic dilated cardiomyopathy and

*Email: claudio.delazzari@ifc.cnr.it

ISSN 1025-5842 print/ISSN 1476-8259 online
© 2011 Taylor & Francis
DOI: 10.1080/10255842.2011.597354
http://www.informaworld.com

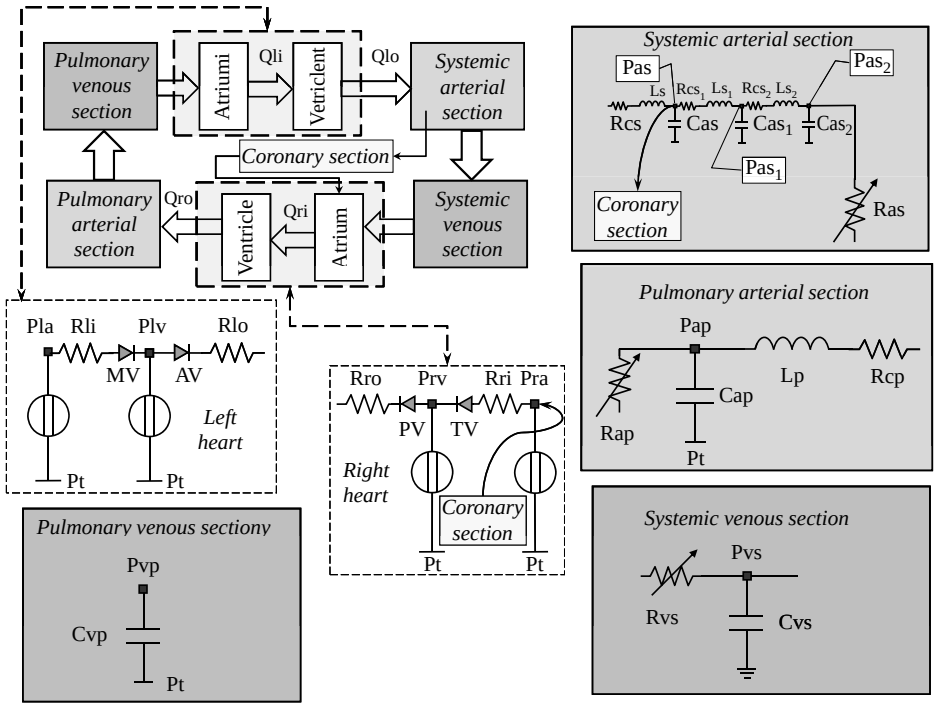

Figure 1. Electric analogue of the numerical simulator. MV (AV) and Rli (Rlo) represent the mitral (aortic) valve. TV (PV) and Rri (Rro) represent the tricuspid (pulmonary) valve. Qli (Qri) is the input flow rate of the left (right) ventricle, Qlo (Qro) is the output flow rate of the left (right) ventricle. Pla (Pra) is the left (right) atrial pressure, Plv (Prv) is the left (right) ventricular pressure, Pas (Pap) is the systemic (pulmonary) arterial pressure, Pvs (Pvp) is the systemic (pulmonary) venous pressure. Pt is the mean intrathoracic pressure.

with IVCD. The software is able to reproduce the haemodynamic patient conditions when the effects of CRT are simulated. Finally, the numerical simulator can predict the trend of CBF–AoP slope, CBF–AoP area and minimum and maximum values of CBF waveform (during the cardiac cycle) in patients treated using CRT.

Materials and methods

The software simulator of the CVS CARDIOSIM© was updated to study the ventricular interactions. This software can reproduce, by haemodynamic point of view, the physiopathological circulatory phenomena and permits to simulate the effects of different mechanical assist devices (De Lazzari et al. 1998; De Lazzari and Ferrari 2007).

CARDIOSIM© has a modular structure that includes the following (Figures 1 and 2):

- the systemic arterial section modelled by a three-cell model (Ferrari et al. 1992; De Lazzari et al. 2009) implemented using, for each cell, a modified windkessel with a characteristic resistance Rcs (Rcs_1 and Rcs_2), an inertance Ls (Ls_1 and Ls_2), a compliance Cas (Cas_1 and Cas_2) and a variable peripheral resistance Ras (Figures 1 and 2);
- the systemic pulmonary section modelled by a modified windkessel with a characteristic resistance Rcp, an inertance Lp, a compliance Cap and a variable peripheral resistance Rap (Figure 1);
- the systemic venous section modelled by a compliance Cvs and the variable resistance Rvs (Guyton et al. 1973; Figure 1);
- the pulmonary venous section modelled by a simple compliance Cvp (Guyton et al. 1973; Figure 1);
- the coronary section (De Lazzari et al. 2009; Figure 2);
- the left and the right heart (Figure 1).

Heart valves are modelled as a diode with a series resistance (Figure 1), assuming the unidirectional way of blood flow.

In the software simulator, the behaviour of both atria is described by variable elastance models (Korakianitis and Shi 2006; De Lazzari et al. 2009) and their mechanical properties are related to the ECG signal schematised as in Figure 3. Ventricular function is reproduced (for both ventricles) using a variable elastance model (Maughan et al. 1987; Sagawa et al. 1988; Korakianitis and Shi 2006). Left time-varying ventricular elastance *elv(t)* is described as a function of the left ventricular systolic elastance *Elvs*, the left ventricular diastolic elastance *Elvd*

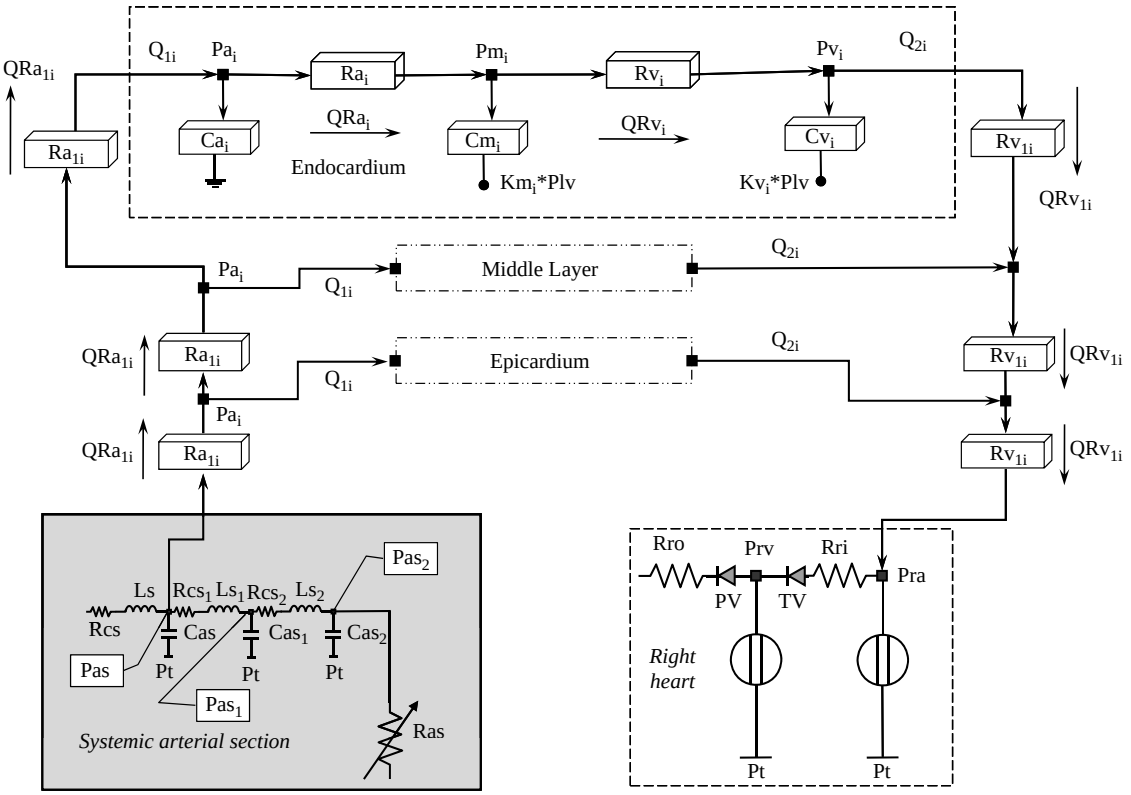

Figure 2. Electric analogue of the coronary circulation. The network is connected to the right atrium and near the output of the left ventricle. The resistances Ra_{1i} (Ra_i) take into account vessels with diameter $>100\,\mu m$ ($<100\,\mu m$).

and the left activation function *alv(t)*:

$$elv(t) = Elvd + \frac{Elvs - Elvd}{2} alv(t), \tag{1}$$

$$alv(t) = \begin{cases} 1 - \cos\left(\frac{t}{T_T}\pi\right), & 0 \le t \le T_T, \\ 1 + \cos\left(\frac{t - T_T}{T_{TE} - T_T}\pi\right), & T_T < t \le T_{TE}, \\ 0, & T_{TE} < t \le T_D, \end{cases} \tag{2}$$

where T_D is the duration of the ECG signal (heart period), T_{TE} is the end of ventricular systole and T_T is the T-wave peak time (Korakianitis and Shi 2006).

In this condition, the instantaneous left ventricular pressure is given by

$$\begin{aligned} Plv(t) &= elv(t) \cdot (Vlv(t) - Vlo) \\ Vlv(t) &= \left(\frac{Plv(t)}{elv(t)}\right) + Vlo, \end{aligned} \tag{3}$$

where *Vlo* is the rest volume of the left ventricle, *Vlv(t)* is the instantaneous left ventricular volume and *Plv(t)* is the instantaneous left ventricular pressure.

This kind of representation can be used to simulate the inter-ventricular dyssynchrony. To simulate also the intra-ventricular dyssynchrony, a model of the ventricular interaction (or 'ventricular interdependence') was implemented through the inter-ventricular septum (Maughan et al. 1987; Sagawa et al. 1988). The concept of ventricular interdependence considers the properties of one ventricle to be a function of the properties of the contralateral ventricle. To model the behaviour of the septum, the time-varying elastance model can be used:

$$e_{SPT}(t) = Ed_{SPT} + \frac{Es_{SPT} - Ed_{SPT}}{2} a_{SPT}(t), \tag{4}$$

where Ed_{SPT} is the septum diastolic elastance, Es_{SPT} is the septum systolic elastance and $a_{SPT}(t)$ is the activation function described in Equation (5):

$$a_{SPT}(t) = \begin{cases} 1 - \cos\left(\frac{t}{T_R}\pi\right), & 0 \le t \le T_R, \\ 1 + \cos\left(\frac{t - T_R}{T_{TE} - T_R}\pi\right), & T_R < t \le T_{TE}, \\ 0, & T_{TE} < t \le T_D, \end{cases} \tag{5}$$

where T_R is the R-wave peak time in the ECG signal.

Instantaneous septum volume ($V_{SPT}(t)$), when $Plv(t) > Prv(t)$, was represented as the volume of shift of the septum from the neutral position towards the right

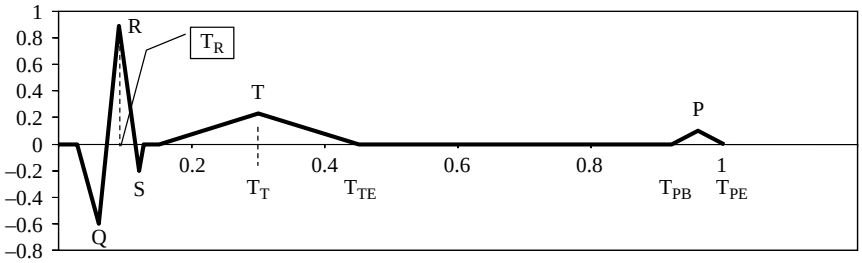

T_R	R wave peak time
T_T	T wave peak time [Ventricular ejection starting]
T_{TE}	Ventricular systole ending
TT-T_{TE}	Ventricular systole duration
T_{PB}	Atrial depolarisation starting
T_{PE}	Atrial depolarisation ending
T_{PB}-T_{PE}	Atrial depolarisation duration

Figure 3. Schematic representation of the ECG signal. The period ($T_T - T_{TE}$) represents the ventricular systole duration and the period ($T_{PB} - T_{PE}$) corresponds to the atrial systole duration.

ventricular lumen (Maughan et al. 1987; Sagawa et al. 1988):

$$V_{SPT}(t) = \frac{Plv(t) - Prv(t)}{e_{SPT}(t)}, \tag{6}$$

where *Prv(t)* is the instantaneous right ventricular pressure.

When $Prv(t) > Plv(t)$, the septum shifts towards the left and the septum volume is given by

$$V_{SPT}(t) = \frac{Prv(t) - Plv(t)}{e_{SPT}(t)}. \tag{7}$$

In this way, the instantaneous left and right ventricular volumes are given by

$$\begin{cases} Vlv(t) = Vlv(t) + V_{SPT}(t), \\ Vrv(t) = Vrv(t) - V_{SPT}(t), \end{cases} \tag{8}$$

where *Vrv(t)* is the instantaneous right ventricular volume.

In Equation (8), substituting *Vlv(t)* in Equation (3) and $V_{SPT}(t)$ in Equation (6) results in:

$$Vlv(t) = \frac{Plv(t)}{elv(t)} \cdot Vlo + \frac{Plv(t) - \Pr v(t)}{e_{SPT}(t)}. \tag{9}$$

From Equation (9), the instantaneous left (right) ventricular pressure becomes:

$$\begin{cases} Plv(t) = \frac{e_{SPT}(t) \cdot elv(t)}{e_{SPT}(t) + elv(t)} \cdot (Vlv(t) - Vlo) + \frac{elv(t)}{e_{SPT}(t) + elv(t)} \cdot Prv(t), \\ Prv(t) = \frac{e_{SPT}(t) \cdot erv(t)}{e_{SPT}(t) + erv(t)} \cdot (Vrv(t) - Vro) + \frac{erv(t)}{e_{SPT}(t) + erv(t)} \cdot Plv(t), \end{cases} \tag{10}$$

where *Vro* is the rest volume of the right ventricle and *erv(t)* is the right time-varying ventricular elastance. In this way, the pressure of the left (right) ventricular chamber is described as a function of its elastance, the pressure and the elastance of the right (left) ventricular chamber.

With the model updated, it is possible to simulate all interactions between the two ventricular chambers.

In the cardiovascular simulator, the coronary network (Figure 2) is developed by lumped parameter representation based on the intramyocardial pump concept (Spaan et al. 1981a, 1981b). The coronary model is subdivided into three parallel sections that represent the endocardial, the middle and the epicardial layers of the left ventricular wall. Each parallel layer is modelled in the same way using RC elements. For each layer, there are an arterial resistance Ra_{1i} (i = endocardium, middle and epicardium layer), an arteriolar resistance Ra_i, a venular resistance Rv_i and a venous resistance Rv_{1i}. Ca_i, Cm_i and Cv_i represent the arteriolar, the capillary and the venular compliance, respectively. Pa_i, Pm_i and Pv_i represent the arteriolar, the capillary and the venous pressures in each layer, respectively. QRa_{1i}, Q_{1i}, QRa_i, QRv_i, QRv_{1i} and Q_{2i} represent the flows in different points of each layer. Km_i and Kv_i are constants and can be assumed different values in each layer. Appendix 1 reports the equations that describe the coronary model.

Q1 The baseline conditions of a patient affected by dilated cardiomyopathy were reproduced from the literature data (De Lazzari et al. 2010), to evaluate the effects induced on CBF and AoP represented on the CBF–AoP plane (Figure 4; Scheel et al. 1989; Di Mario et al. 1994; Krams et al. 2004; De Lazzari et al. 2009). Different ECG times, intra-ventricular and inter-ventricular delays were used to achieve such a goal. These data are related to patients with moderate or severe HF, with an IVCD, treated by CRT.

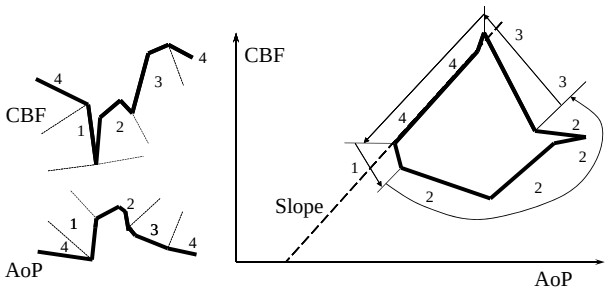

Figure 4. Schematic CBF, AoP waveforms and CBF–AoP loop. The curves are subdivided into four different phases along the cardiac cycle. Systole being represented by segments 1 and 2 and diastole by segments 3 and 4. Segment 1 corresponds to the ventricular isometric contraction. Segment 2 corresponds to the ejection period. Segment 3 corresponds to the relaxation and rapid ventricular filling. Finally, segment 4 corresponds to the late diastolic period in which coronary resistance becomes constant and flow linearly declines with the coronary driving pressure. The slope (dashed line) of this portion of the CBF–AoP loop has been considered an index of maximal coronary conductance, capable of assessing the haemodynamic significance of coronary stenosis (Di Mario et al. 1994).

Using these data, we simulated the effects of different intra-ventricular and inter-ventricular times.

To reproduce the baseline and the conditions induced by CRT with different intra-ventricular and inter-ventricular times, the parameters of the numerical simulator were set as follows:

- Data (De Lazzari et al. 2010) of the systolic (AoP_S) and diastolic (AoP_D) aortic pressures were reproduced changing automatically Ras using a dedicated algorithm implemented in the software (Ferrari et al. 1992).
- Es_{SEPT}, Ed_{SEPT} and *Elvs* (*Ervs*) were set to place the left ventricular loop in the pressure–volume plane according to the end systolic volume (ESV) and end diastolic volume (EDV) data (De Lazzari et al. 2010). To place the left ventricular loop, it has also been assumed that the left ventricular end systolic pressure (Pes) can be approximated with mean AoP value (Sagawa et al. 1988; De Lazzari et al. 2010).

Table 1. Literature data used to perform the numerical simulations.

	HR (beats/min)	AoP_S (mm Hg)	AoP_D (mm Hg)	AoP (mm Hg)	ESV (EDV) (ml)	Inter-ventricular delay (ms)	Intra-ventricular delay (ms)	EF (%)
				Before CRT				
#1	76	90	60	70	192 (213)	36*	70	10
#2	75	110	60	77	139 (201)	28	50	31
#3	68	110	70	83	105 (160)	50	60	34
#4	80	130	85	100	110 (170)	45	60	35
#5	70	100	70	80	78 (105)	37*	67*	25
#6	64	110	80	90	115 (160)	30	50	28
#7	65	100	60	73	144* (186*)	37	50	23
				Within 6 months since CRT				
#1	75	95	60	72	130 (169)	25*	20	23
#2	75	110	70	83	145 (215)	10	20	33
#3	64	100	60	73	86 (153)	20	25	44
#4	70	110	70	83	90 (150)	25	20	40
#5	80	100	60	73	46 (85)	0	6	46
#6	70	120	75	90	94 (154)	9	20	39
#7	70	110	70	83	120 (171)	9*	20*	30

Note: The symbol '*' next to the data indicates that the literature data were published incorrectly.

	Before CRT			Within 6 months since CRT		
	QRS (ms)	QT (ms)	PQ (ms)	QRS (ms)	QT (ms)	PQ (ms)
#1	180	340	180	120	370	160
#2	140	420	220	160	420	180
#3	150	410	180	140	420	180
#4	150	420	FA	130	430	FA
#5	120	400	180	120	420	180
#6	140	410	160	130	410	160
#7	140	400	160	130	410	160

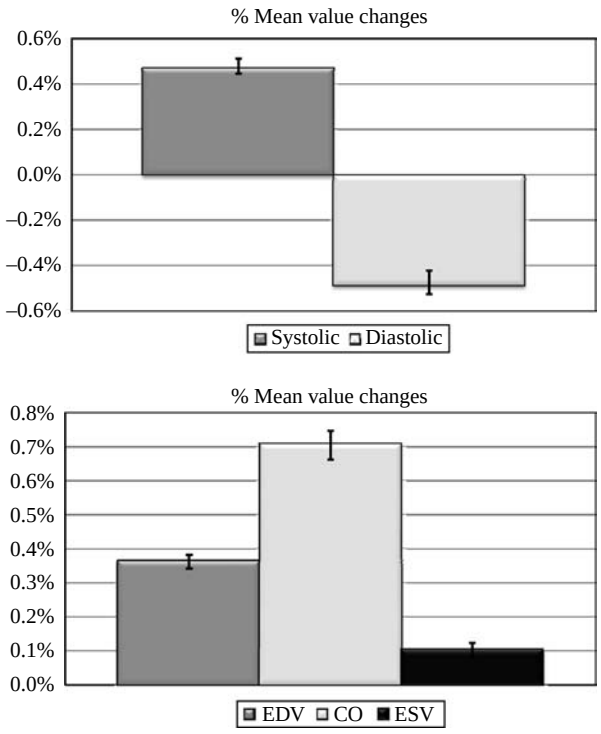

Figure 5. Percentage change calculated on the mean percentage changes between the simulated and the observed data before and within 6 months since CRT. The upper panel shows the diastolic and systolic percentage mean changes evaluated on the AoP ($p < 0.0001$). The lower panel shows the EDV, CO and ESV percentage mean changes ($p < 0.0001$).

- Heart rate (HR), QT, PQ and QRS times, ejection fraction (EF), inter-ventricular and intra-ventricular delay were set using the literature data (De Lazzari et al. 2010).

Table 1 shows the data (De Lazzari et al. 2010) used during the simulations. In Table 1, the symbol '*' attached to the data indicates that the literature data were published incorrectly. The correct values are reported in the table.

Results

In Figure 5, the upper panel shows for AoP the percentage change calculated on the mean percentage changes evaluated from the simulated and observed data (reported in Table 1) before and within 6 months since CRT. The lower panel shows for EDV, ESV and cardiac output (CO), the percentage change calculated on the mean percentage changes evaluated from the simulated and observed data (reported in Table 1) before and within 6 months since CRT. In the observed data, the CO was estimated multiplying the stroke volume and the HR. The 'p value' of 5% was considered statistically significant. Figure 6 shows one of the different possible outputs produced by the CARDIOSIM© software simulator. The figure reports graphical and numerical data for two different cardiocirculatory conditions regarding patient 1. For this patient, the baseline conditions (A) and the conditions after CRT (B) are reproduced using data reported in Table 1. The figure represents the left ventricular loops (on the pressure–volume plane), the CBF–AoP loops and the mean pressure (flow) values calculated during the cardiac cycle. For each CBF–AoP loop, the slope (Di Mario et al. 1994) is also reproduced. Finally, EDV (Ved), ESV (Ves) and stroke volume (SV) are presented for both ventricles.

Finally, Figure 7 shows for the seven patients the CBF results obtained using the software simulator. In all panels, the dark (white) bars represent the positive (negative) percentage changes, when the patients are switched from the baseline to assisted (CRT) conditions. The upper left (right) panel shows the percentage changes in the minimum (maximum) CBF value evaluated by comparing simulated baseline and assisted (within 6 months since CRT) data. The lower left (right) panel shows the percentage changes in the CBF–AoP slope (in CBF–AoP area) evaluated comparing simulated baseline data with the data obtained simulating the patient conditions after about 6 months since CRT. The CBF–AoP slope (Figure 4) can give information on the maximal diastolic coronary conductance.

Discussion

The data presented in Figure 5 show that the software simulator can reproduce the cardiocirculatory conditions, in terms of haemodynamic parameters, of different patients with different intra-ventricular and inter-ventricular delays. The study of patients affected by advanced systolic HF treated using CRT permits to evaluate the effects of IVCD. The results presented in Figure 5 show that the simulator reproduces quite faithfully haemodynamic variables such as systolic (diastolic) AoP, end systolic (diastolic) left ventricular volume and CO, in both baseline and after CRT conditions (in patients affected by HF). In relation to aortic systolic pressure, the upper panel of figure shows that the simulator overestimates the literature data by an average of about 0.47%. For the aortic diastolic pressure, the software underestimates the literature data by an average of about 0.5%. The lower panel of Figure 5 shows that simulated EDV, ESV and CO were overstimated when compared with those observed by 0.37% (EDV), 0.1% (ESV) and 0.71% (CO), respectively. Figure 6 reproduces the baseline conditions and the conditions after CRT of patient 1 obtained using the software simulator. It is possible to observe the effects produced by different ECG times and intra-ventricular and inter-ventricular delays on the CBF–AoP (in figure produced by the software Qcor-Pas) loops. In patient 1, the reduction of QRS duration from 180 to 120 ms (after CRT), the reduction of PQ duration from 180 to 160 ms and the increase in the QT duration from 340 to 370 ms

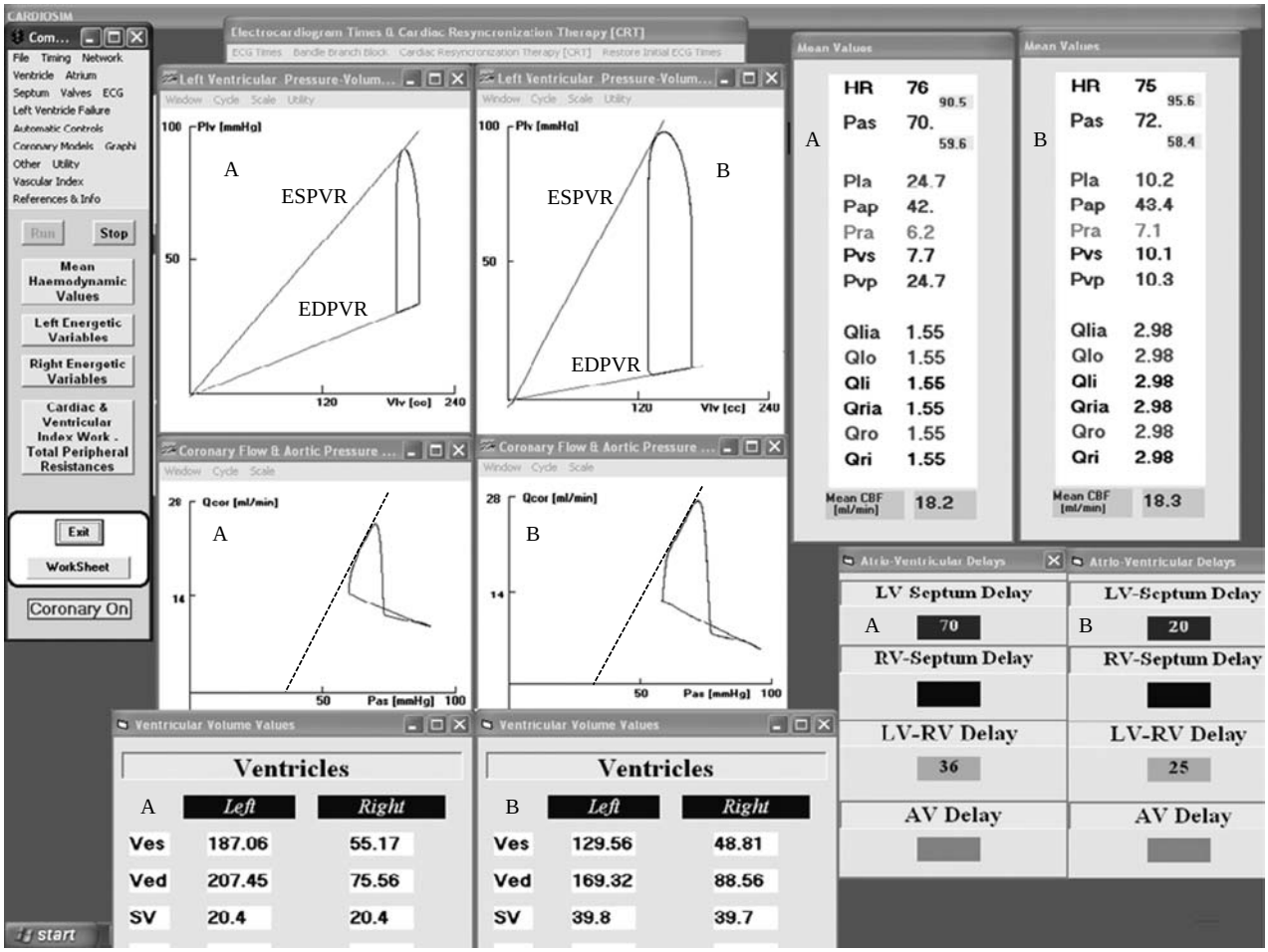

Figure 6. Screen output produced by the CARDIOSIM© software. Panel A (B) shows patient 1 baseline (within 6 months since CRT) conditions reproduced from the data presented in Table 1. The upper graphical window reproduces the ventricular loops in the left pressure–volume plane. ESPVR (EDPVR) is the end systolic (diastolic) pressure–volume relationship. Plv (Vlv) is the left ventricular pressure (volume). The lower graphical window shows the CBF–AoP loops. Qcor and Pas in the software simulator represent the CBF and the systemic arterial pressure (AoP), respectively. The lower numerical panel shows for both ventricles the end systolic volume (Ves), the end diastolic volume (Ved) and the stroke volume (SV). In the right numerical panel are the reported HR and mean pressures and flow rate values calculated during the cardiac cycle. Pla (Pra) is the mean left (right) atrial pressure. Pap is the mean pulmonary arterial pressure. Pvs (Pvp) is the mean venous systemic (pulmonary) pressure. Qlia (Qria) is the mean left (right) input atrial flow rate. Qlo (Qro) is the mean left (right) ventricular output flow rate. Qli (Qri) is the mean left (right) ventricular input flow rate. The two right-lower numerical panels report the left (LV), right (RV) ventricular delays during baseline (A) and within 6 months since CRT (B) conditions. Finally, the left panel shows the software simulator commands panel.

together with the reduction in inter-ventricular delay from 36 to 25 ms and intra-ventricular delay from 70 to 36 ms produce different effects on CBF–AoP loop.

By switching from baseline (A) to CRT (B) conditions, it is possible to observe an increase (a reduction) in the maximum (minimum) value of CBF, an increase in the CBF–AoP loop area and a variation in CBF–AoP slope. Figure 6 shows that the mean CBF during the cardiac cycle remains unchanged. These results show that the changes induced in QRS, QT, PQ, intra-ventricular and inter-ventricular times produce changes in the duration of the different phases of the loop represented in Figure 4.

The upper left panel of Figure 7 shows that the percentage variations on minimum value of the CBF induced by the CRT simulation assumes positive and negative values in patients. It should be noted that during the simulations (from baseline to CRT), the values of coronary resistances and compliances were not changed. In physiological point of view, CBF is regulated by different mechanisms depending on the driving pressure, the coronary resistances and the compliances (Valzania et al. 2008). In this study, the effects of driving pressure have been taken into account when the CRT was applied, in fact in the coronary model (Figure 2) some compliances are connected to the left ventricular pressure. Instead, during the simulations, the coronary resistances and compliances values were not changed in the transition from baseline simulation compared with CRT. In any case,

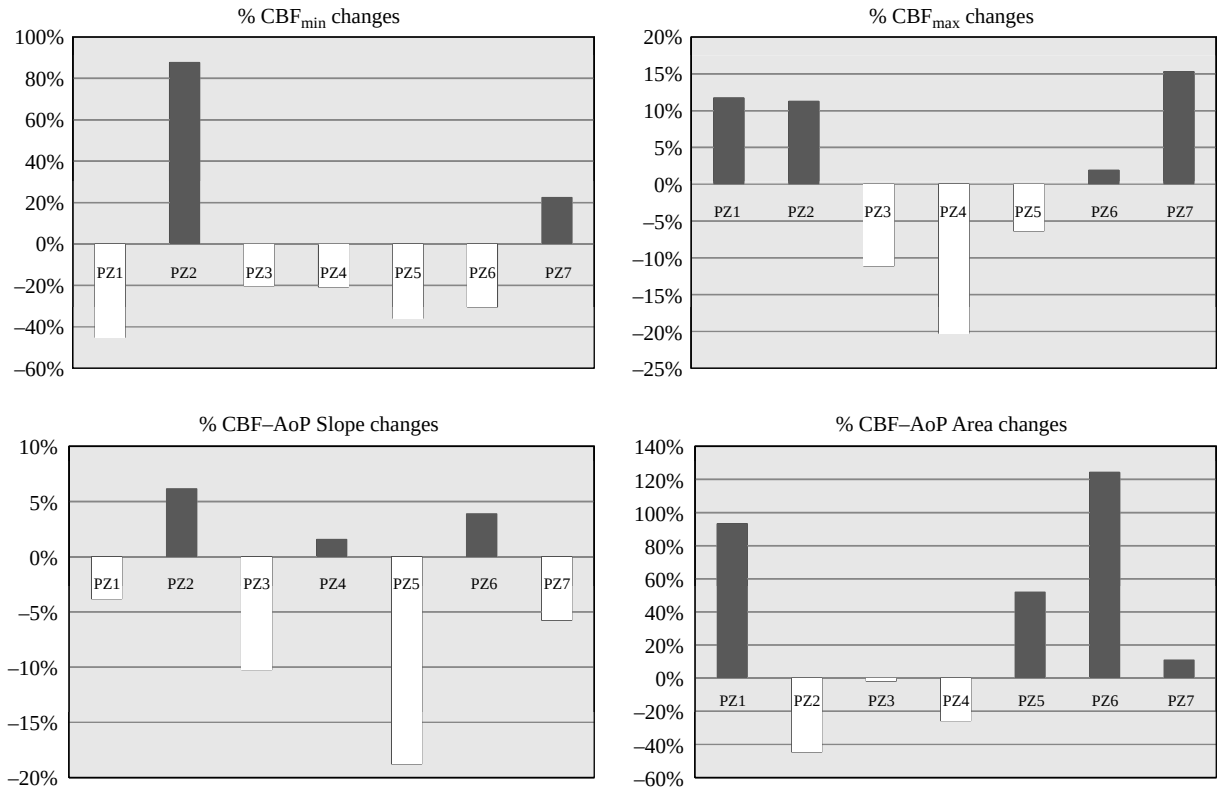

Figure 7. CBF results produced by software simulator. For the seven patients in all panels, the figure shows the percentage changes between the baseline data and the data after the CRT, calculated from the literature data. The upper left (right) panel shows the percentage changes in the minimum (maximum) CBF. The lower left (right) panel shows a bar diagram reporting the percentage changes of the CBF–AoP slope (CBF–AoP area).

patients 2 and 7 present an increase in the minimum value of CBF when the software simulator switches from baseline to CRT conditions. These two patients, together with patients 1 and 6, present an increase in the maximum value of CBF (upper right panel). In the lower left panel, the percentage variation of the CBF–AoP slope can give information on the maximal diastolic coronary conductance and presents a reduction in four patients after CRT simulation. Also these results must be interpreted bearing in mind that the simulations made to reproduce the patient circulatory conditions before and after CRT were made without changing the values of coronary resistances and compliances.

The CBF–AoP representation can be proposed as an indirect parameter to evaluate the function of the coronary circulation. An abnormal coronary flow reserve value may also reflect changes in coronary or systemic haemodynamics as well as changes in extravascular coronary resistance (e.g. increased intramyocardial pressure). From this perspective, the numerical simulator can be a valuable tool for assessing the effects of cardiac resynchronisation.

Finally, analysing the lower right panel of Figure 7, we observe that also the percentage variations in CBF–AoP area assume an increase in patients 1, 5, 6 and 7, when CRT simulation is applied. A reduction is registered in patients 2, 3 and 4. The controversial results, regarding the effects of CRT on CBF, presented in Figure 7, are in accordance to *in-vivo* results presented in the literature (Nelson et al. 2000; Lindner et al. 2005; Flevari et al. 2006). In line with literature results, in patients with different pathological conditions (as ischaemic HF patients or non-ischaemic patients), the CRT produces different effects on CBF.

Conclusions

The numerical model implemented inside CARDIOSIM© allows to reproduce the interaction between the septum and the left (right) ventricular free wall to evaluate the effects on CBF. The software simulator can reproduce the pathological conditions of patients affected by HF, with IVCD, and it is able to reproduce the haemodynamic conditions when CRT is applied. The numerical simulator results regarding haemodynamic variables (in baseline and CRT conditions) are in accordance with literature data. Also the controversial results on CBF in the presence of CRT, obtained using the software simulator, are consistent with those described in the literature.

Considering that limited data are available regarding non-invasive measurements of CBF in HF patients treated using CRT (Yildirim et al. 2007) and considering that techniques such as Doppler catheterisation and coronary sinus thermodilution (used for measuring CBF in humans) are invasive and affected by serious limitations, the use of a numerical simulator, as described in this work, may help to understand the effects on CBF produced by CRT, making sure to work on a substantial number of patients with similar pathological conditions.

References

De Lazzari C, D'Ambrosi A, Tufano F, Fresiello L, Garante M, Sergiacomi R, Stagnitti F, Caldarera CM, Alessandri N. 2010. Cardiac resynchronization therapy: could a numerical simulator be a useful tool in order to predict the response of the biventricular pacemaker synchronization? Eur Rev Med Pharmacol Sci. 14(11):969–978.

De Lazzari C, Darowski M, Ferrari G, Clemente F. 1998. The influence of left ventricle assist device and ventilatory support on energy-related cardiovascular variables. Med Eng Phys. 20(2):83–91.

De Lazzari C, Di Molfetta A, Fresiello L. 2009. Comprehensive models of cardiovascular and respiratory system. Their mechanical support and interactions. Chapter 2, Heart Models. New York: Nova Science. p. 49–59.

De Lazzari C, Ferrari G. 2007. Right ventricular assistance by continuous flow device: a numerical simulation. Methods Inf Med. 46(5):530–537.

De Lazzari C, Ferrari G, Mimmo R, Tosti G, Ambrosi D. 1994. A desk top computer model of the circulatory system for heart assistance simulation: effect of an LVAD on energetic relationships inside the left ventricle. Med Eng Phys. 16(2): 97–103.

De Lazzari C, Neglia D, Ferrari G, Bernini F, Micalizzi M, L'Abbate A, Trivella MG. 2009. Computer simulation of coronary flow waveforms during caval occlusion. Methods Inf Med. 48(2):113–122.

Di Mario C, Kramas R, Gil R, Serruys PW. 1994. Slope of the instantaneous hyperemic diastolic coronary flow velocity–pressure relation. A new index for assessment of the physiological significance of coronary stenosis in humans. Circulation. 90:1215–1224.

Edvardsen T, Rodevand O, Endresen K, Ihlen H. 2005. Interaction between left ventricular wall motion and intraventricular flow propagation in acute and chronic ischemia. Am J Physiol Heart Circ Physiol. 289: H732–H737.

Ferrari G, De Lazzari C, Mimmo R, Tosti G, Ambrosi D. 1992. A modular numerical model of the cardiovascular system for studying and training in the field of cardiovascular physiopathology. J Biomed Eng. 14:91–107.

Flevari P, Theodorakis G, Paraskevaidis I, Kolokathis F, Kostopoulou A, Leftheriotis D, Kroupis C, Livanis E, Kremastinos DT. 2006. Coronary and peripheral blood flow changes following biventricular pacing and their relation to heart failure improvement. Europace. 8(1):44–50.

Ghio S, Constantina C, Klersyb C, Serioa A, Fontana A, Campana C, Tavazzi L. 2004. Interventricular and intraventricular dyssynchrony are common in heart failure patients, regardless of QRS duration. Eur Heart J. 25(7): 571–578.

Guyton AC, Jones CE, Coleman TG. 1973. Circulatory physiology: cardiac output and its regulation. Computer analysis of total circulatory function and of cardiac output regulation. Philadelphia (PA): WB Saunders. p. 285–301.

Kalogeropoulos A, Georgiopoulou V, Howell S, Pernetz M, Fisher M, Lerakis S, Martin R. 2008. Evaluation of right intraventricular dyssynchrony by two-dimensional strain echocardiography in patients with pulmonary arterial hypertension. J Am Soc Echocardiog. 21(9):1028–1034.

Kamdar R, Frain E, Warburton F, Richmond L, Mullan V, Berriman T, Thomas G, Tenkorang J, Dhinoja M, Earley M, Sporton S, Schilling R. 2010. A prospective comparison of echocardiography and device algorithms for atrioventricular and interventricular interval optimization in cardiac resynchronization therapy. Europace. 12(1):84–91.

Korakianitis T, Shi Y. 2006. A concentrated parameter model for the human cardiovascular system including heart valve dynamics and atrioventricular interaction. Med Eng Phys. 28:613–628.

Krams R, Ten Cate FJ, Carlier SG, van der Steen AFW, Serruys PW. 2004. Diastolic coronary vascular reserve: a new index to detect changes in the coronary microcirculation in hypertrophic cardiomyopathy. J Am Coll Cardiol. 43: 670–677.

Lindner O, Vogt J, Kammeier A, Wielepp P, Holzinger J, Baller D, Lamp B, Hansky B, Körfer R, Horstkotte D, Burchert W. 2005. Effect of cardiac resynchronization therapy on global and regional oxygen consumption and myocardial blood flow in patients with non-ischaemic and ischaemic cardiomyopathy. Eur Heart J. 26:70–76.

Maughan WL, Sunagawa K, Sagawa K. 1987. Ventricular systolic interdependence: volume elastance model in isolated canine hearts. Am J Physiol Heart Circ Physiol. 253: H1381–H1390.

Nelson GS, Berger RD, Fetics BJ, Talbot M, Spinelli JC, Hare JM, Kass DA. 2000. Left ventricular or biventricular pacing improves cardiac function at diminished energy cost in patients with dilated cardiomyopathy and left bundle-branch block. Circulation. 102(25):3053–3059.

Rinaldi CA, Bucknall CA, Gill JS. 2002. Beneficial effects of biventricular pacing in a patient with hypertrophic cardiomyopathy and intraventricular conduction delay. Heart. 87(6):e6, doi:10.1136/heart.87.6.e6.

Sagawa K, Maughan L, Suga H, Sunagawa K. 1988. Contraction and the pressure–volume relationships. New York: Oxford University Press.

Scheel KW, Mass H, Williams SE. 1989. Collateral influence on pressure-flow characteristics of coronary circulation. Am J Physiol Heart Circ Physiol. 257:H717–H725.

Slinker BK, Glantz SA. 1986. End systolic and end-diastolic ventricular interaction. Am J Physiol. 251:H1062–H1075.

Spaan JA, Nreuls NP, Laird JD. 1981a. Diastolic–systolic coronary flow differences are caused by intramyocardial pump action in the anesthetized dog. Circ Res. 49:584–593.

Spaan JA, Nreuls NP, Laird JD. 1981b. Forward coronary flow normally seen in sistole is the result of both forward and concealed back flow. Basic Res Cardiol. 76:582–586.

Valzania C, Gadler F, Winter R, Braunschweig F, Brodin LA, Gudmundsson P, Boriani G, Eriksson MJ. 2008. Effects of cardiac resynchronization therapy on coronary blood flow: evaluation by transthoracic Doppler echocardiography. Eur J Heart Fail. 10:514–520.

Yildirim A, Soylu O, Dagdeviren B, Ergelen M, Celik S, Zencirci E, Tezel T. 2007. Cardiac resynchronization improves coronary blood flow. Tohoku J Exp Med. 211:43–47.

Appendix 1

Equations used to solve the analogue network representing the coronary circulation.

$$QRa_{1\mathrm{MID}} = \frac{Pa_{\mathrm{MID}} - Pa_{\mathrm{EPI}}}{Ra_{1\mathrm{MID}}}, \quad Q_{1\mathrm{EPI}} = QRa_{1\mathrm{EPI}} - QRa_{1\mathrm{MID}},$$

$$QRa_{1\mathrm{EPI}} = \frac{Pas + Pt - Pa_{\mathrm{EPI}}}{Ra_{1\mathrm{EPI}}}, \quad \frac{\mathrm{d}Pa_{\mathrm{EPI}}}{\mathrm{d}t} = \frac{Q_{1\mathrm{EPI}} - QRa_{1\mathrm{EPI}}}{Ca_{\mathrm{EPI}}},$$

$$QRa_{\mathrm{MID}} = \frac{Pa_{\mathrm{MID}} - (Pm_{\mathrm{MID}} + Km_{\mathrm{MID}} \cdot Plv)}{Ra_{\mathrm{MID}}}, \quad \frac{\mathrm{d}}{\mathrm{d}t}(Pa_{\mathrm{EPI}} - Km_{\mathrm{EPI}} \cdot Plv) = \frac{QRa_{\mathrm{EPI}} - QRv_{\mathrm{EPI}}}{Cm_{\mathrm{EPI}}},$$

$$QRv_{\mathrm{EPI}} = \frac{(Pa_{\mathrm{EPI}} - Pv_{\mathrm{EPI}})}{Rv_{\mathrm{EPI}}}, \quad \frac{\mathrm{d}}{\mathrm{d}t}(Pv_{\mathrm{EPI}} - Kv_{\mathrm{EPI}} \cdot Plv) = \frac{QRv_{\mathrm{EPI}} - Q_{2\mathrm{EPI}}}{Cv_{\mathrm{EPI}}},$$

$$QRv_{1\mathrm{EPI}} = \frac{(Pv_{\mathrm{EPI}} - (Pra + Pt))}{Rv_{1\mathrm{EPI}}}, \quad QRa_{1\mathrm{MID}} = \frac{Pa_{\mathrm{EPI}} - Pa_{\mathrm{MID}}}{Ra_{1\mathrm{MID}}} - QRa_{1\mathrm{ENDO}},$$

$$QRv_{1\mathrm{MID}} = \frac{(Pv_{\mathrm{MID}} - Pv_{\mathrm{EPI}})}{Rv_{1\mathrm{MID}}},$$

$$Q_{2\mathrm{MID}} = QRv_{1\mathrm{MID}} - Q_{2\mathrm{SUB}}, \quad Q_{2\mathrm{EPI}} = QRv_{1\mathrm{EPI}} - QRv_{1\mathrm{MID}},$$

$$QRa_{\mathrm{MID}} = \frac{(Pa_{\mathrm{MID}} - Pm_{\mathrm{MID}})}{Ra_{\mathrm{MID}}}, \quad \frac{\mathrm{d}Pa_{\mathrm{MID}}}{\mathrm{d}t} = \frac{Q_{1\mathrm{MID}} - QRa_{\mathrm{MID}}}{Ca_{\mathrm{MID}}},$$

$$QRv_{\mathrm{MID}} = \frac{(Pm_{\mathrm{MID}} - Pv_{\mathrm{MID}})}{Rv_{\mathrm{MID}}}, \quad \frac{\mathrm{d}}{\mathrm{d}t}(Pm_{\mathrm{MID}} - Km_{\mathrm{MID}} \cdot Plv) = \frac{QRa_{\mathrm{MID}} - QRv_{\mathrm{MID}}}{Cm_2},$$

$$\frac{\mathrm{d}}{\mathrm{d}t}(Pv_{\mathrm{MID}} - Kv_{\mathrm{MID}} \cdot Plv) = \frac{QRv_{\mathrm{MID}} - Q_{2\mathrm{MID}}}{Cv_{\mathrm{MID}}}, \quad Q_{2\mathrm{SUB}} = \frac{(Pv_{\mathrm{SUB}} - Pv_{\mathrm{MID}})}{Rv_{\mathrm{SUB}}},$$

$$Q_{1\mathrm{SUB}} = \frac{Pa_{\mathrm{MID}} - Pa_{\mathrm{SUB}}}{Ra_{1\mathrm{SUB}}}, \quad QRa_{\mathrm{SUB}} = \frac{(Pa_{\mathrm{SUB}} - Pm_{\mathrm{SUB}})}{Ra_{\mathrm{SUB}}},$$

$$\frac{\mathrm{d}Pa_{\mathrm{SUB}}}{\mathrm{d}t} = \frac{Q_{1\mathrm{SUB}} - QRa_{\mathrm{SUB}}}{Ca_{\mathrm{SUB}}}, \quad QRv_{\mathrm{SUB}} = \frac{(Pm_{\mathrm{SUB}} - Pv_{\mathrm{SUB}})}{Rv_{\mathrm{SUB}}},$$

$$\frac{\mathrm{d}}{\mathrm{d}t}(Pv_{\mathrm{SUB}} - Kv_{\mathrm{SUNB}} \cdot Plv) = \frac{QRv_{\mathrm{SUB}} - Q_{2\mathrm{SUB}}}{Cv_{\mathrm{SUB}}}, \quad \frac{\mathrm{d}}{\mathrm{d}t}(Pm_{\mathrm{SUB}} - Km_{\mathrm{SUB}} \cdot Plv) = \frac{QRa_{\mathrm{SUB}} - QRv_{\mathrm{SUB}}}{Cm_{\mathrm{SUB}}}.$$